Power Closed-loop Control of Switched Reluctance Generator for High Efficiency Operation

Zhenguo Li *, Dongdong Gao *, and Jin-Woo Ahn **

Abstract –This paper describes a control method of turn-on/off angles to improve the efficiency of the switched reluctance generator(SRG) with a power closed-loop control system, and the inner-loop of the system is current hysteresis control. The SRG control system is constituted by the PI power controller and the two-level current hysteresis controller. By measuring and analyzing the system losses of different reference powers, speeds and turn-on/off angles, selection strategy of optimal turn-on/off angles is discussed. The proposed method is simple, reliable, and easy to achieve.

Keywords: Switched reluctance generator, Current control, Power closed-loop control, High-efficiency operation

1. Introduction

The switched reluctance machine can be operated as motor and generator modes according to the different turn-on/off angles. Both of the two operating modes can be considered as dual relation[1]. However, there are some differences between the two operating modes, especially when high-performance is needed.

There are so many advantages of the SRG, such as low-manufacturing cost, fault tolerance, operation in high speed and temperature, and application in harsh environment for the rugged and simple construction[1]. Typical applications include aerospace power systems, hybrid electric vehicles, wind-turbine application and so on. The objective of SRG control is normally to track the output power and keep the DC-link voltage at a desired value with high-efficiency, low-torque ripple, and low-acoustic noise. These control objectives can be optimized by appropriately adjusting the turn-on/off of the angles.

Current chopping control and single pulse control are adopted respectively as inner loop to hold-on DC-link voltage in [2] and [3]. Moreover, optimal turn-on/turn-off angles can be chosen by analysis of the system efficiency and torque ripple in [2], while in [3] by a ratio of two flux, the flux where entire-overlapped stator and rotor poles start to detach and the max flux linkage. Based on measured magnetization curve, optimal on/off angle can be obtained by analysis of output power and system efficiency under a series of different on/off angles in [4]. Specific application of SRG in wind power generation is described in [5].

In this paper, efficient operation of SRG in power closed-loop system is the main objective, and optimal on/off angle can be chosen by reference power and rotor speed. The system is composed of PI controller and two-level hysteresis current controller. By lots of testing and analysis of system losses under different reference powers, rotor speeds and on/off angles, optimal on/off angles can be obtained. The proposed method is simple, reliable and easy to realize.

2. Analysis of power closed-loop control of SRG

The control diagram for power closed-loop system is shown in Fig.1, which consists of power converter, DC electrical source, controller and position sensor. Voltage equations of each phase are described as following.

$$u_{ph} = Ri_{ph} + L(i_{ph},\theta)\frac{di_{ph}}{dt} + \frac{\partial L(i_{ph},\theta)}{\partial\theta} i_{ph}\omega_r \qquad (1)$$

where subscript *ph* is one of these phases, the phase inductance L is the function of the rotor position and θ the phase current i_{ph}, and $e_{ph}=(\partial L/\partial\theta)\cdot i_{ph}\omega_r$ is rotational electromotive force.

In the generator mode, each phase is excited after overlap of stator and rotor poles, where $(\partial L/\partial\theta) < 0$, as a result $e_{ph} < 0$.

* Key Lab of Power Electronics for Energy Conservation and Motor Drive of Hebei Province, Yanshan University, Qinhuangdao 066004, China (lzg@ysu.edu.cn; 916078991@qq.com)

** Department of Mechatronics Engineering, Kyungsung University, Busan 608-736, Korea (jwahn@ks.ac.kr)

Received ; Accepted

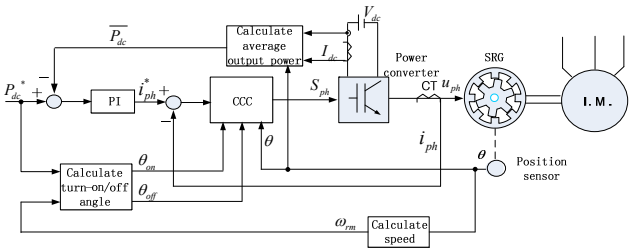

Fig. 1. Block diagram of 8/6-pole SRG with power closed-loop control system

2.1 Power converter and Average output power

The power converter for SRG have two modes: self-excitation and separated excitation modes. Fig. 2 shows the self-excitation power converter for 8/6-pole SRG, in which R is load resistance, full bridge rectifier with diodes and filter capacitor C form a circuit to hold-on DC-link voltage when SRG generates electricity.

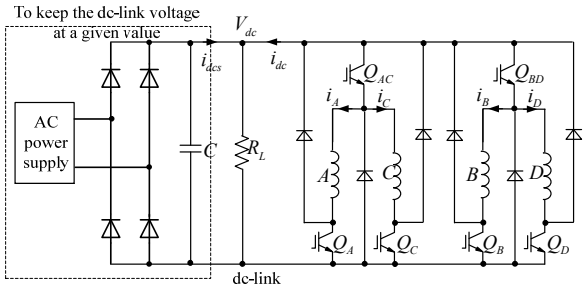

Fig. 2. Power converter with a 8/6 four-phase SRG

When phase resistance is ignored, the derivative of the phase current can be achieved from (1) .

$$\frac{di_{ph}}{dt}=\frac{1}{L}(-e_{ph}+u_{ph}) \tag{2}$$

where the phase voltage depends on the state of the switch tubes on each bridge legs, including V_{dc},0,-V_{dc} corresponding to three stages in up and down bridge legs.

The u_{ph} decides energy transfer direction between SRG and DC source, when the phase current was excited. In addition, the change of phase current depends on u_{ph} and DC-link voltage as in (2). When the operation of the SRG is in the middle-low speed, u_{ph} is smaller than V_{dc}, current can be adjusted by DC-link voltage chopping control, when the operation is in high speed, u_{ph} is bigger than V_{dc}, and phase current is out of control during generation period.

Electric power fluctuates periodically as inherent characteristic in SRG, the period is $T=\theta_{sk}/\omega_r$ to turn stroke angle. Hence, controlled object should be average power in power control as following

$$\overline{P}_{dc}=\frac{1}{T}\int_0^T V_{dc}i_{dc}dt=\frac{V_{dc}}{\theta_{sk}}\int_{\theta_{on}}^{\theta_{on}+\theta_{sk}} i_{dc}d\theta \tag{3}$$

where, $\theta_{sk}=2\pi/(mp_r)$, m and p_r is the number of phases and poles respectively.

2.2 Hysteresis Current Control

Fig.3 is the ideal curves of phase, current, voltage, inductance and flux linkage under two-level hysteresis current controller. During generator stage, two-level hysteresis current control operates with soft chopping by *0* and V_{dc}, so the average phase voltage is smaller than DC link voltage, and balance out eph. Turn-on angle θ_{on}, turn-off angle θ_{off} and reference current i_{ph}^* are needed in hysteresis current controller. θ_r is the position when phase current reaches to the reference current, which varies with θ_{on} and i_{ph}^*. From Fig.2 and 3, the relation between i_{dc} and i_{ph} can be achieved as following.

$$i_{dc}=\sum S_{ph}i_{ph} \tag{4}$$

where S_{ph} is switch state, including 1,0,-1, respectively corresponding to turn on up and down bridge legs, turn on only one bridge leg, and turn off the whole bridge legs.

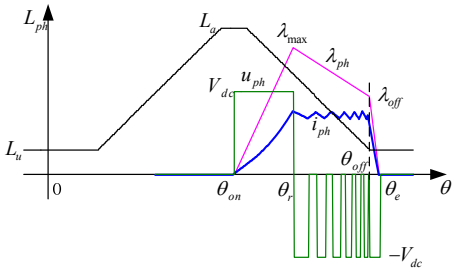

Fig. 3. Typical waveforms of two-level hysteresis current control

2.3 The Average Input Mechanical Power and Efficiency

In the system, instantaneous input torque is the sum of each phase torque, and fluctuates periodically just like average input power, the period is $T=\theta_{sk}/\omega_r$. Therefore average torque is applied to calculate efficiency as following.

$$\begin{aligned}\overline{T}_e&=\frac{1}{T}\int_0^T\sum\left[\frac{1}{2}\frac{\partial L(i_{ph},\theta)}{\partial\theta}i_{ph}^2\right]dt\\&=\frac{1}{\theta_{sk}}\int_{\theta_{on}}^{\theta_{on}+\theta_{sk}}\sum\left[\frac{1}{2}\frac{\partial L(i_{ph},\theta)}{\partial\theta}i_{ph}^2\right]d\theta\end{aligned} \tag{5}$$

The average input mechanical power is in (6).

$$\overline{P}_m=\overline{T}_e\cdot\omega_r \tag{6}$$

From (3) and (6), efficiency is calculated as follow.

$$\eta = \frac{\overline{P}_{dc}}{\overline{P}_m} \tag{7}$$

2.4 Theoretical Analysis of System losses

System losses in the system include copper loss, iron loss, mechanical loss, switching loss and so on, among which the most important are copper loss and core loss. Copper loss depends on phase current rms in (8).

$$P_{cu} = mI_{ph\_rms}{}^2 R \tag{8}$$

Phase current rms $I_{ph\_rms}{}^2$ is calculated in (9) by Fig.3.

$$I_{ph\_rms} = \sqrt{\frac{1}{\theta_{rpp}} \int_{\theta_{on}}^{\theta_e} i_{ph}^2 d\theta} \tag{9}$$

where $\theta_{rpp}=2\pi/p_r$ is rotor pole pitch.

In Fig.3, phase current is viewed as linear during dwell period $(\theta_{dwell}=\theta_r-\theta_{on})$ and tail period $(\theta_{tail}=\theta_e-\theta_{off})$, then (9) is simplified as follow.

$$I_{ph\_rms} = \sqrt{\frac{(\theta_e-\theta_{on})+(\theta_{off}-\theta_r)}{2\theta_{rpp}}} \cdot I_{ph} \tag{10}$$

where I_{ph} is peak phase current, which is approximately equal to reference current i_{ph}^* in SRG power loop system

Iron loss includes magnetic hysteresis loss and eddy current loss, which is related to the maximum MMF and frequency of alternating magnetic field. Since flux waveforms are non-sinusoidal and flux harmonic spectra differ in various parts of the magnetic circuit, iron loss is not uniformly distributed in the core. An approximate formulae based on Steinmetz equation could be used for iron loss calculation in a SRG [6].

$$P_{Fe} = c_h f B^{a+bB} + c_e \left(\frac{dB}{dt}\right)^2 \tag{11}$$

where f is the stroke frequency, c_h and c_e are the hysteresis and eddy-current loss coefficients, respectively, and a and b are coefficients that could be determined from the loss curves using a curve fitting procedure.

3. Efficiency optimization of SRG power closed-loop control system

Turn-on/off angles are chosen to improve system efficiency or to decrease torque ripple for the system.

3.1 Relation Between Efficiency and Turn-on Angle

Fig.4 shows the phase current and flux linkage curves with different turn-on angles. For the constant average input torque, peak current increases from Iph to Iph1 while turn-on angle from θ_{on} to θ_{on1}. If magnetic saturation and dwell, tail current are neglected, the relation can be achieved from (5) as follow.

$$\overline{T}_e \propto (\theta_{off}-\theta_r)\cdot I_{ph}^2 \tag{12}$$

Known from (10) and (12), though Iph increases, I_{ph_rms} and copper loss of SRG approximately remains unchanged. As shown in Fig.4, the inductance value on θ_r position is in proportion to the length of power generation period $(\theta_{on}-\theta_r)$, so peak flux is in proportion to $(\theta_{on}-\theta_r)$ I_{ph}, and then peak flux decreases along with iron loss.

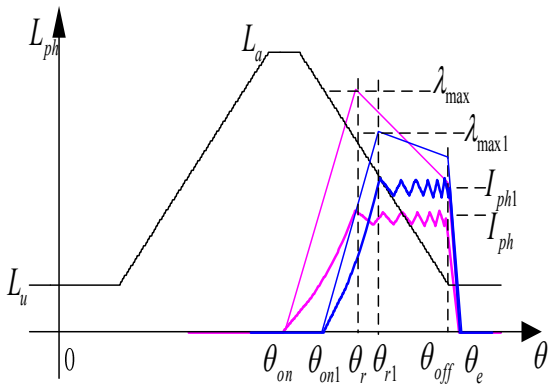

Fig. 4. Phase current and flux with various turn-on angles

By the analysis mentioned above, if magnetic saturation, dwell and tail current are neglected, system efficiency is improved as θ_{on} increasing. In fact, SRG operates in magnetic saturation, and dwell, tail current can't be neglected, so I_{ph_rms} increases along with θ_{on}, and then copper loss increases. Fig.5 shows the curves of phase current rms and peak flux linkage with different turn-on angles and constant $\theta_{off}=52^\circ$ in the power loop system for a 8/6-pole SRG. As shown in Fig.5, the system outputs needed electric power only operating in given turn-on angle, current rms increases more quickly and peak flux decreases more slowly with turn-on angle increasing. Fig.6 gives the loss curve of the system. The system loss is the discrepancy between the input power of prime mover and the output electric power of SRG, Containing the prime mover loss. The prime mover is a three-phase squirrel cage induction motor. From the results, we can find that the efficiency changes obviously with the turn-on angle increases, and there is an optimal opening angle.

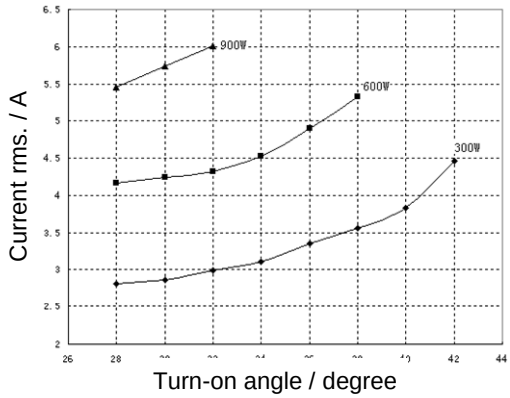

(a) Phase current rms

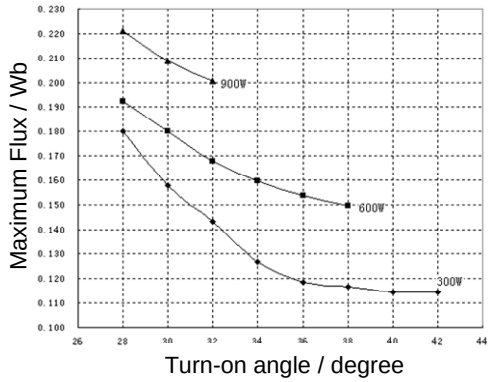

(b) Peak flux linkage

Fig. 5. Phase current rms and peak flux linkage with various turn-on angles

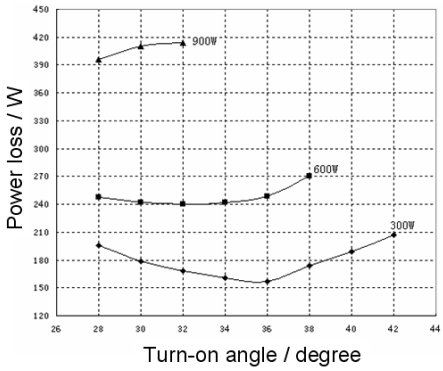

Fig. 6. The total system losses when Turn-on angle change (including loss of the prime mover)

3.2 Relationship Between Efficiency and Turn-off Angle

Fig.7 shows the various phases current and flux linkage curves with different turn-off angles in the system. When the average input torque remains unchanged and turn-off angle decreases from θ_{off} to θ_{off1}, peak current increases from I_{ph} to I_{ph1}. If magnetic saturation and dwell, tail current are neglected, I_{ph_rms} and copper loss of SRG approximately remains unchanged just like the analysis of various turn-on angles above. As shown in Fig.6, the position of phase current reaching to reference current is constant for constant θ_{on}; peak flux λ_{max} and iron loss increases along with I_{ph} increasing.

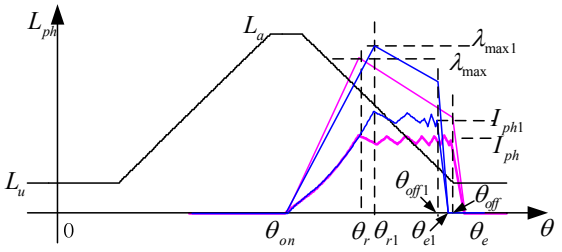

Fig. 7. Phase current and flux linkage with various turn-off angles

By the analysis mentioned above, if magnetic saturation, dwell and tail current are neglected, system efficiency drops with decreasing θ_{off}. When without neglecting magnetic saturation, and dwell, tail current, I_{ph_rms} decreases along with increasing θ_{off}, and then copper loss decreases. Fig.8 shows the curves of *Iph_rms* and λ_{max} with different turn-off angles and constant $\theta_{on}=28^\circ$ in the system for a 8/6-pole SRG. Phase current rms and peak flux change a little with turn-on angle decreasing. The total system losses as shown in Fig.9. The system losses contain the prime mover loss, it is similar to Fig.6. From the results, we can find that the change of efficiency is not too obvious with the turn-on angle increases. So, the high efficiency operation of the system should not be used to change the turn-off angle

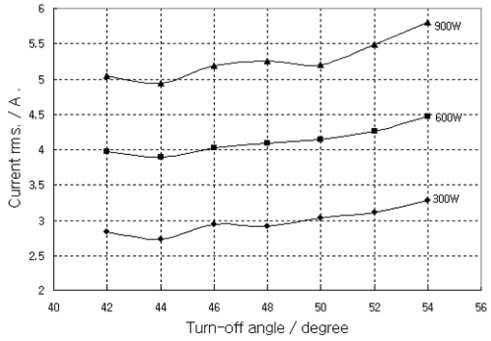

(a) Phase current rms

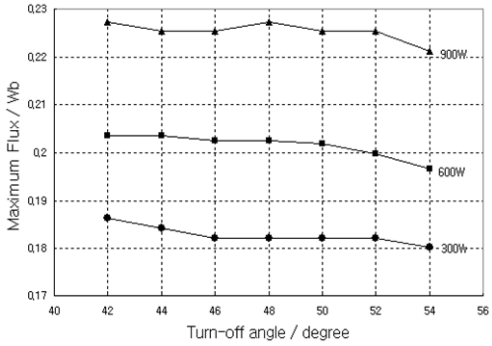

(b)Peak flux linkage

Fig. 8. Phase current rms and peak flux linkage with various turn-off angles

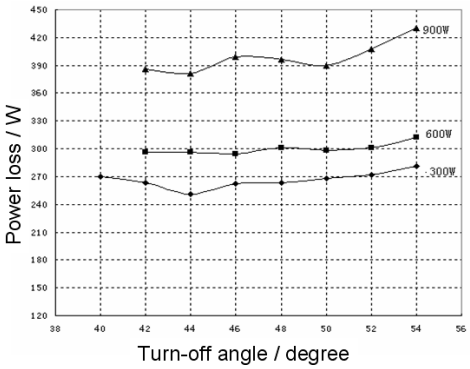

Fig. 9. The total system losses when Turn-off angle change (including loss of the prime mover)

3.3 Strategy to choose the optimal turn-on/off angles

By the analysis mentioned above, the change of turn-off angle has a little contribution to system efficiency. So the advisable method for optimal efficiency is to adjust turn-on angle with constant turn-off angle in the system.

4. Experimental results and analysis

The experiment set-up of the SRG system is shown in Fig.10; main parameters are 2kW、300V、four-phase、8/6-pole. The prime mover applies a 1.5kW four-pole three-phase induction motor. In experiment, the TMS320F28335 DSP-150MHz produced by Texas Instruments is used, and the cycle for the inner hysteresis current control is 25μs. In addition, considering the actual DC grid voltage, the DC-link voltage is set to 200V.

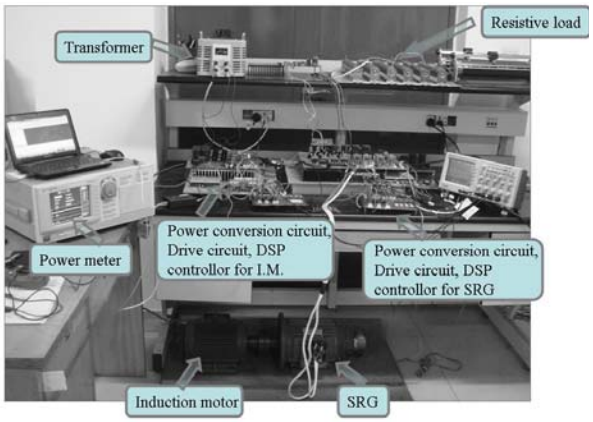

Fig. 10. Experiment set-up

Fig.11 and 12 show the experimental results under the step reference power respectively for 0→1kW, and 0→1kW→300W. For the SRG, the average output power is calculated and controlled every *360/(4*6)=15°*. Clearly the system has a well dynamic response with power PI controller, and the system reaches steady state just after several control-cycles.

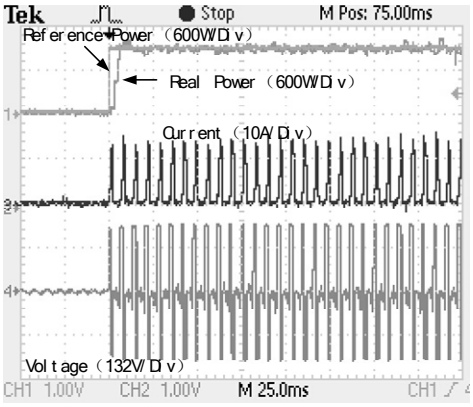

(a) Reference power, current and voltage

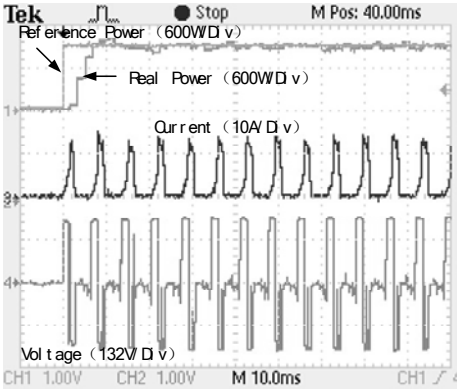

(b) Detail view of figure

Fig. 11. Experimental results under step reference power from 0 to 1kW

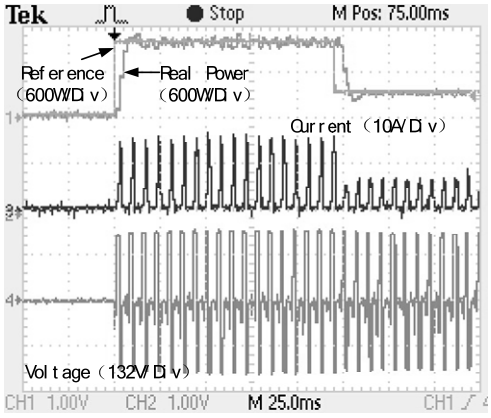

(a)Reference power, current and voltage

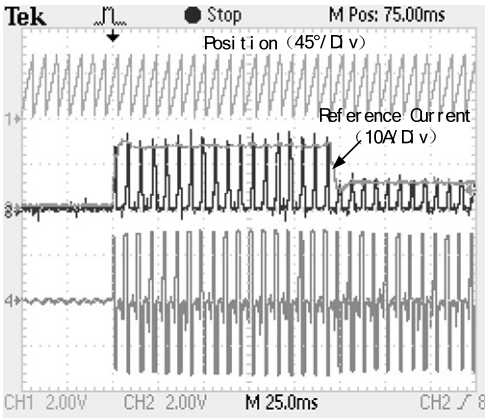

(b) Detail view of figure

Fig. 12. Experimental results under step reference power from 0 to 1kW, to 300W

5. Conclusion

In this paper, efficient operation of SRG in power closed-loop system is the main objective. The system losses and efficiency are discussed, and the relation between system losses and turn-on and off angles is discussed by theoretical analysis and experiment.

The selection strategy of optimal turn-on and off angles are introduced, SRG power closed-loop system which PI power controller and the two-level current hysteresis controller are setup and tested. The proposed method is simple, reliable, and easy to achieve.

Acknowledgements

This work was supported by the National Research Foundation of Korea(NRF) grant funded by the Korea Government(MEST) (No. 2012-0005022), and by the Natural Sciences Foundation of Hebei Province of China (No. E2010001263).

References

[1] T. J. E. “Miller, Electronic Control of Switched Reluctance Machines,” Oxford, U.K.: Newnes,Christos Mademlis, Iordanis.

[2] Kioskeridis, “Optimizing Performance in Current-Controlled Switched Reluctance Generators,” IEEE Trans. on energy conversion, Vol.20, No.3, pp.556-565, 2005.

[3] Iordanis Kioskeridis, Christos Mademlis, “Optimal Efficiency Control of Switched Reluctance Generators,” IEEE Trans. on power electronics, Vol.21, No.4, pp.1062-1072, 2006.

[4] Jawad Faiz, Reza Fazai, “Optimal Excitation Angles of a High Speed Switched Reluctance Generator by Efficiency Maximization,” EPE-PEMC 2006, pp.287-291, 2006.

[5] Roberto Cardenas, Ruben Pena, Marcelo Perez, Jon Clare, Greg Asher, Patrick Wheeler, “Control of a Switched Reluctance Generator for Variable-Speed Wind Energy Applications,” IEEE Trans. on Energy Conversion, Vol. 20, No. 4, pp. 781-791, 2005.

[6] Y. Hayashi and T. J. E. Miller, “A new approach to calculate core losses in the SRM,” IEEE Trans. Ind. Appl., vol. 31, no. 5, pp. 1039–1046, Sep./Oct. 1995.

[7] Zhenguo Li, Jian Ma, Chunjiang Zhang, Dong-Hee Lee and Jin-Woo Ahn, “Research of Switched Reluctance wind power generator system Based on variable Generation voltage converter,” ICEMS 2010, pp.418421, 2010.

Zhenguo Li received the B.S. degree in electric machinery and electrical apparatus from Shenyang University of Technology, Shenyang, China, in 1994, and the M.S. and Ph.D. degrees in mechatronics engineering from Pukyong National University, Busan, Korea, in 2001 and 2005, respectively. He is currently with Yanshan University, Qinhuangdao, China, as an Associate Professor. His major research field is advanced electrical motor control.

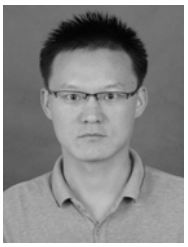

Dongdong Gao received B. E n g degree in Biomedical Engineering from Yanshan University , Qinhuangdao, China, in 2010. His research interest is advanced electrical motor control.

Jin-Woo Ahn was born in Busan, Korea, in 1958. He received his B.S., M.S., and Ph.D. degrees in Electrical Engineering from Pusan National University, Pusan, Korea, in 1984, 1986, and 1992, respectively.

He has been with Kyungsung University, Busan, Korea, as a professor in the Department of Mechatronics Engineering since 1992. He was a visiting researcher in the Speed Lab at Glasgow University, U.K., a visiting professor in the Dept. of ECE and WEMPEC at the University of Wisconsin-Madison, USA, and a visiting professor in the Dept. of ECE at Virginia Tech from July 2006-June 2007. He was the director of the Advance Electric Machinery and Power Electronics Center. He also has been the director of the Smart Mechatronics Advanced Research and Training Center from Aug. 2008 to July 2011 and the Senior Easy Life Regional Innovation System since July 2008, President of Korea Regional Innovation System Association since December 2011 which are authorized by the Ministry of Knowledge Economy, Korea. He is the author of five books including SRM, the author of more than 150 papers and has more than 20 patents. His current research interests are advanced motor drive systems and electric vehicle drives. He has been the Editor-in-Chief of JICEMS.

Dr. Ahn received several awards including the Best Paper Award from the Korean Institute of Electrical Engineers in 2002 and 2011, The Korean Federation of Science and Technology Society in 2003, Korean Institute of Power Electronics in 2007, Park Min-Ho Prize in 2009, Busan Science & Technology Prize in 2011 and Ministerial Citation of Ministry of Knowledge Economy in 2011, respectively. He is a Fellow of the Korean Institute of Electrical Engineers, a member of the Korean Institute of Power Electronics and a senior member of the IEEE.